Fast pulsing dynamics of a vertical-cavity surface-emitting laser operating in the low-frequency fluctuation regime

M. Sciamanna,[1] C. Masoller,[2] F. Rogister,[1] P. Mégret,[1] N. B. Abraham,[3] and M. Blondel[1]

[1]*Service d'Electromagnétisme et de Télécommunications, Faculté Polytechnique de Mons, Boulevard Dolez 31, B-7000 Mons, Belgium*
[2]*Instituto de Fisica, Facultad de Ciencias, Universidad de la Republica, 11400 Montevideo, Uruguay*
[3]*DePauw University, Greencastle, Indiana 46135-0037, USA*

We analyze the dynamics of a vertical-cavity surface-emitting laser with optical feedback operating in the low-frequency fluctuation regime. By focusing on the fast pulsing dynamics, we show that the two linearly polarized modes of the laser exhibit two qualitatively different behaviors: they emit pulses in phase just after a power dropout and they emit pulses out of phase after the recovery process of the output power. As a consequence, two distinct statistical distributions of the fast pulsating total intensity are observed, either monotonically decaying from the noise level or peaked around the mean intensity value. We further show that gain self-saturation of the lasing transition strongly modifies the shape of the intensity distribution.

The light polarization of vertical-cavity surface-emitting lasers (VCSELs) has received a lot of interest, considering its possibility to switch between two orthogonal linearly polarized (LP) modes (x and y) [1]. VCSELs are also very sensitive to delayed optical feedback, which may arise, e.g., from back reflections at the cleaved end of a fiber [2]. The interplay between time delay and polarization competition is responsible for new dynamics [3–7], not present in edge-emitting lasers (EELs), which might lead to interesting applications in all optical signal handling [7,8].

In this Brief Report, we study the feedback-induced low-frequency fluctuation (LFF) regime in VCSELs. The LFF regime is characterized by sudden dropouts of the laser output, at random time intervals, combined with the emission of sharp pulses on a much shorter time scale [9]. Studies of the LFF regime in VCSELs are scarce [10–12], in contrast to EELs. An important question, which has not yet been investigated, concerns the correlation properties of the two LP modes of the VCSEL when it operates in the LFF regime. To answer this question, we analyze the fast pulsing dynamics in the two LP modes, on the basis of a simple extension of the San Miguel, Feng, and Moloney (SFM) model [13] to account for isotropic optical feedback. Our model for VCSELs is simple while it retains the physics that results in predictions consistent with experiments on LFF in VCSELs [11]. We unveil interesting correlation properties in the LP mode intensities, with coexistence of in-phase pulsing and slower antiphase dynamics. We further show that the total intensity may exhibit two qualitatively different statistical distributions, depending on the correlation between the LP mode intensities and/or the gain self-saturation of the lasing transition. Our results motivate new experiments on the LFF regime in VCSELs, with a sub-nanosecond resolution.

In the framework of SFM model [13,14], the carrier density is decomposed into two subsets of carriers with spin up and down, respectively, defining two radiation channels associated with circularly polarized light. We have extended the SFM model to account for external polarization preserving optical feedback and nonlinear saturation of the gain of the lasing transition. In the circularly polarized basis of the

field, our equations are written as

$$\dot{E}_\pm = \kappa(1+i\alpha)[(N\pm n)F_\pm - 1]E_\pm - (\gamma_a + i\gamma_p)E_\mp$$
$$+ fE_\pm \exp(-i\omega_0\tau) + \sqrt{\beta_{sp}(N\pm n)}\xi_\pm, \quad (1)$$

$$\dot{N} = -\gamma[N-\mu+(N+n)F_+|E_+|^2+(N-n)F_-|E_-|^2], \quad (2)$$

$$\dot{n} = -\gamma_s n - \gamma[(N+n)F_+|E_+|^2-(N-n)F_-|E_-|^2], \quad (3)$$

where $E_\pm$ are the left and right circularly polarized components of the slowly varying optical field. N takes into account the total population difference between conduction and valence bands and n corresponds to the difference between the two distinct subpopulation inversion densities which couple separately to the emission of left and right circularly polarized light. κ is the field decay rate in the cavity, α is the phase-amplitude coupling factor, γ is the carrier relaxation rate. $\gamma_s \equiv \gamma + 2\gamma_j$, where γ_j is a coupling rate between the two circularly polarized radiation channels, which models different microscopic relaxation mechanisms that equilibrate the spin of carriers [13]. γ_p (γ_a) is the intensity of linear birefringence (dichroism), per intracavity round-trip time. β_{sp} is the spontaneous emission rate and $\xi_\pm$ are independent white noises of unitary variance and zero mean value. μ is the normalized injection current ($\mu = 1$ at threshold). f is the feedback rate and $\omega_0\tau$ is the feedback phase, with ω_0 being the solitary laser frequency at the lasing threshold and τ being the external-cavity round-trip time. $F_\pm$ are the two gain saturation terms, defined as $F_\pm = 1 - \epsilon|E_\pm|^2$, where ϵ is a gain self-saturation coefficient. $F_\pm$ account for the nonlinear saturation of the two lasing transitions. Since $E_\pm$ couple separately to their respective radiation channel, we assume that each radiation channel saturates independently, and therefore no cross-saturation terms are included in the rate equations when written in the circularly polarized basis [11,15]. Moreover, we consider that each lasing transition saturates with the same rate ϵ. We omit cross-saturation terms not only for simplicity but also because we find nu-
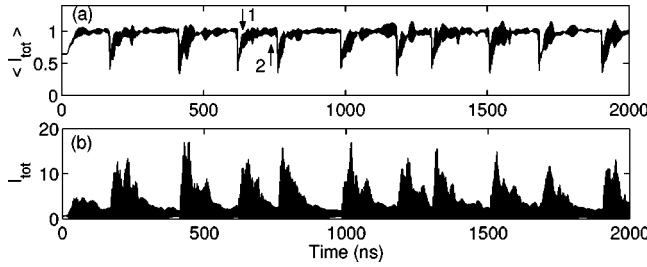
FIG. 1. Time traces of I_{tot} in the LFF regime, after averaging on 1 ns (a) or on 10 ps (b), in order to unveil the fast pulsing dynamics underlying the slow LFF. Parameters are $\mu=1.5$, $f=80$ GHz, $\kappa=300$ ns^{-1}, $\gamma=1$ ns^{-1}, $\gamma_s=10$ ns^{-1}, $\gamma_a=-0.1$ ns^{-1}, $\gamma_p=4$ ns^{-1}, $\alpha=3$, $\tau=3$ ns, $\omega_0\tau=6$ rad, $\beta_{sp}=10^{-4}$ ns^{-1}, and $\epsilon=0$.

merically that the inclusion of cross-saturation terms in $F_\pm$ (of the same order of magnitude than self-saturation terms) does not significantly modify the LFF polarization dynamics.

We have modeled the delayed feedback from the external cavity by following the Lang-Kobayashi (LK) approach [16], which considers only one round-trip term in the external cavity. The high reflectivity of the output mirror in VCSELs might however justify to the inclusion of multiple external-cavity round-trip terms in the field equation (1), as first suggested by Law and Agrawal [17] and later argued by Giudici *et al.* [11]. However, LFF dynamics reported in Ref. [11], which was obtained from a model that includes all round trips in the external cavity, also occurs in the model (1)–(3) that considers a simple LK approximation [12]. Thus, the relevance of multiple external-cavity round trips in the dynamics of VCSELs operating in the LFF regime remains to be elucidated.

Figure 1(a) illustrates power dropouts in the total intensity $I_{tot}\equiv|E_+|^2+|E_-|^2$, obtained numerically from Eqs. (1)–(3). The time trace has been averaged to be 1 ns. Figure 1(b) shows the total intensity dynamics as it could be observed with a detector of much larger bandwidth (100 GHz). The total intensity exhibits pulses which underly the slow LFF dynamics of Fig. 1(a).

Figure 2 displays the dynamics for a short time interval selected just after a power dropout [during the recovery process, see arrow 1 in Fig. 1(a)]. Figures 1(b) and 1(c) show the intensities in the two LP modes, i.e., $I_{x,y}\equiv|E_{x,y}|^2$, where $E_x\equiv(E_++E_-)/\sqrt{2}$ and $E_y\equiv-i(E_+-E_-)/\sqrt{2}$. The LP modes exhibit a train of pulses starting from a zero value with a repetitive pattern at the external-cavity delay time (see arrow in Fig. 2). We point out that the pulses are emitted by the LP modes in a synchronous way, such that both modes fire pulses at the same time. However, when one LP mode fires a large pulse, the other LP mode usually fires a smaller pulse, hence unveiling a partial antiphase dynamics at a larger time scale than the one of the pulsating dynamics. Due to this modal behavior, the total intensity also exhibits trains of pulses starting from the noise level, with a similar behavior relative to the LP modes. In order to gain insight into the LP mode dynamics, we have used the product of the modal intensities as it was proposed by Vaschenko *et al.* [18]; see Fig. 2(d). The product of LP mode intensities just after a
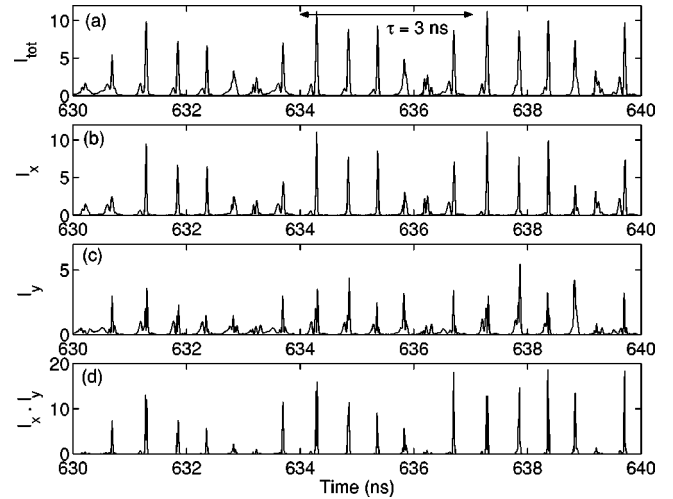
FIG. 2. Fast pulsing dynamics in the total power (a), the *x*-LP mode (b), and the *y*-LP mode (c) for a time span indicated by arrow 1 in Fig. 1(a), i.e., just after a total power dropout. The product of the LP mode intensities is shown in (d).

dropout event is sharply peaked with a large number of zero-value time intervals, indicating an emission of pulses in a synchronous, but often an alternating, way.

Figure 3 is the same as Fig. 2, but for a short time span selected after the total power has recovered [arrow 2 in Fig. 1(a)]. The LP modes still emit pulses, with an almost repetitive pattern at multiples of the external-cavity round-trip time, but the pulses have broadened and are no longer synchronous. Due to this exchange of energy between the LP modes, the behavior of the total intensity is very different from the one of the individual modes, and also different from that we could observe just after a power dropout. The product of modal intensities presented in Fig. 3(d) is also very different from the one in Fig. 2(d): it is lower [compare the vertical scale with the one in Fig. 2(d)], denser, and shows only short zero-value time spans.

The coexistence of in-phase and out-of-phase pulses in
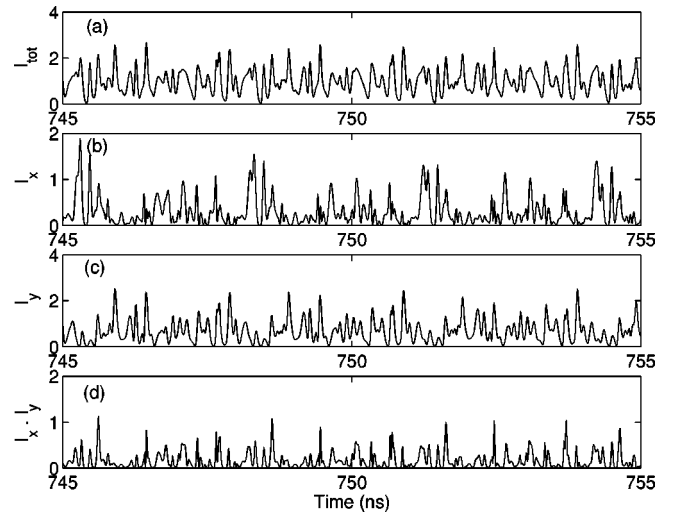
FIG. 3. Same as Fig. 2, but for a time span indicated by arrow 2 in Fig. 1(a), i.e., after the total power has been recovered.
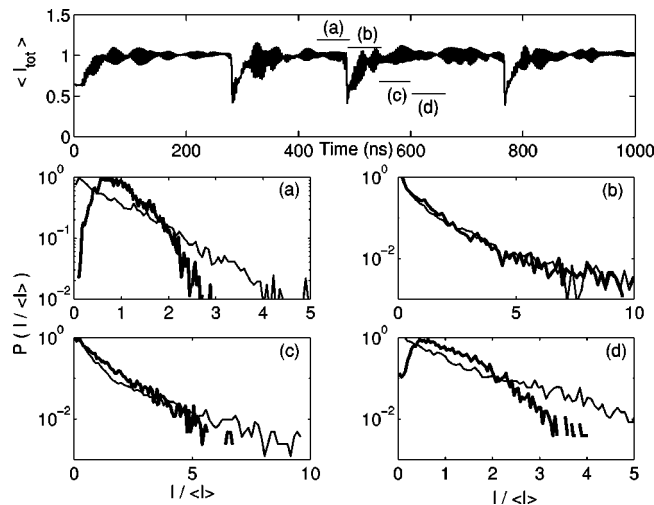
FIG. 4. Statistical distributions of I_x (thin line) and I_{tot} (thick line) for four 60 ns time spans taken before and after a total power dropout: (a) the 420–480 ns time interval (before the power dropout), (b) the interval 480–540 ns (during the recovery process), (c) the interval 540–600 ns, and finally (d) the interval 600–660 ns (before the next power dropout event).

FIG. 5. Temporal traces of I_{tot} and the corresponding statistical distributions for $\mu = 1.5$ and two different values of the feedback rate: $f = 60$ GHz (a),(b); $f = 80$ GHz (c),(d). The other parameters are the same as in Fig. 1. The thick (thin) line in (b),(d) refers to I_{tot} (I_x).

the LP modes of a VCSEL operating in the LFF regime is qualitatively similar to the one reported in EELs [18–20], if one relates the LP modes to the longitudinal modes of the EELs. This is remarkable if one takes into account the fact that the mode interaction mechanisms among the longitudinal modes of an EEL are very different from the mode interaction mechanisms of the LP modes of a VCSEL.

Next, we study the statistics of the intensity pulses. In Fig. 4 we have plotted the statistical distributions of I_x (thin line) and I_{tot} (thick line), as they can be observed for different time spans of 60 ns (20 round-trips in the external cavity) situated just before a power dropout [Figs. 4(a) and 4(d)], and during the recovery process [Figs. 4(b) and 4(c)]. The intensity is normalized by its mean value, $\langle I \rangle$, and its statistic is plotted on a logarithmic scale, for clarity. The statistic of I_y is not shown, since it is similar to that of I_x. The statistical distribution of I_x is always monotonically decaying, independently of the temporal abscissa relative to the power dropout. This is due to the fact that the individual LP modes always emit pulses. In contrast, Figs. 4(a) and 4(d) show that for the situation before a power dropout the statistical distribution of I_{tot} is sharply peaked around the mean intensity value. Immediately after a dropout [Figs. 4(b) and 4(c)], the statistical distribution of I_{tot} becomes monotonically decaying with a long tail at high intensities, indicating the emission of very high intensity pulses. This again confirms that, just after a power dropout (during the recovery process), the most probable value of I_{tot} is around the noise level, while after the recovery process it is around its mean value.

Figure 4 displays statistics of fast pulsing intensity for specific time intervals chosen either before or just after a power dropout. However, an experimental analysis of the fast pulsing polarization dynamics in VCSELs would record the statistics on the basis of a large number of time intervals
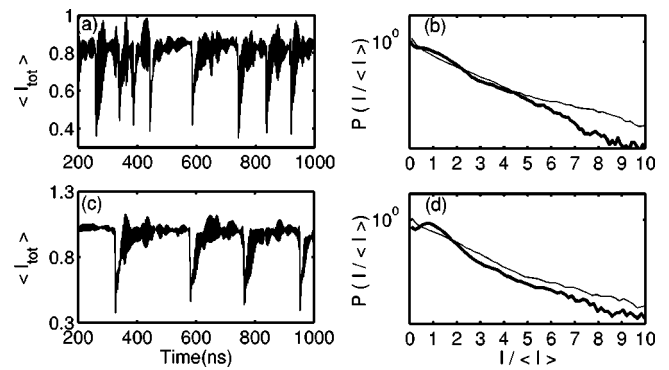
that are not correlated with the power dropouts. Our preceding discussion allows us to conclude that the statistics of the fast pulsing total intensity, computed on a large number of uncorrelated time intervals, will strongly depend on the relative proportion of the in-phase to the out-of-phase pulses emission in the LP modes, hence will depend on how frequently power dropouts occur; see Fig. 5. Figure 5 shows, on the right column, the statistical distributions of the instantaneous total and modal intensities and on the left column, the corresponding total averaged intensity, for two different values of the feedback rate. The statistics of the y-LP mode intensity is not shown, since it is similar to that of the x-LP mode intensity. The statistics have been computed on a long time trace that includes a few tens of power dropouts. In both cases, the statistical distributions of the LP modes decrease monotonically, indicating the emission of pulses departing from the noise level, and the most probable intensity value is very low. In the case of Figs. 5(a) and 5(b), the statistical distribution of the total intensity is also monotonically decaying, indicating that the total intensity and the LP modes behave similarly. In this case, the predominant dynamical behavior is the in-phase pulses emission in the LP modes. When increasing the feedback rate [Figs. 5(c) and 5(d)], the spacing between power dropouts increases [21], and a small peak appears in the statistical distribution of the total inten-
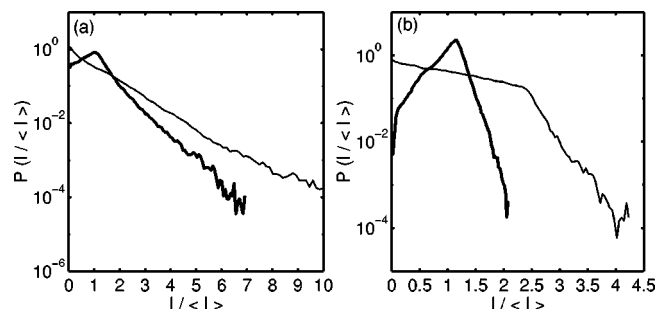
FIG. 6. Statistical distributions of I_{tot} (thick line) and I_x (thin line) for the same parameters as in Figs. 5(a),(b) and for $\epsilon = 0.01$ (a) and $\epsilon = 0.1$ (b).

sity around the mean intensity value. This result is due to the contribution of the out-of-phase dynamics in the LP modes, which is more important here than in Figs. 5(a) and 5(b).

Our conclusions remain valid in a large range of parameters, including large variations of γ_s ($10 \text{ ns}^{-1} \leqslant \gamma_s \leqslant 300 \text{ ns}^{-1}$). We also find that the dropouts in total intensity are less frequent as γ_s increases, hence an increase of γ_s yields a total intensity statistics more peaked around its mean value. The available experiments on LFF in VCSELs are efficiently modeled with a small γ_s [11,12], but they can also be reproduced with another model other than SFM, which does not include spin-relaxation mechanisms [12]. It is therefore not possible to conclude from these experiments which γ_s value should be included in our simulations. The relevance of spin-relaxation mechanisms also needs to be elucidated in solitary VCSELs [1,22].

Finally, we analyze the influence of the gain saturation coefficient ϵ on the intensity statistics. Figure 6 shows the intensity statistics for $\epsilon = 0.01$ [Fig. 6(a)] and $\epsilon = 0.1$ [Fig. 6(b)]. Clearly, for larger ϵ the distribution of the total intensity becomes more peaked around the mean intensity value. Indeed, since gain saturation strongly damps the relaxation oscillations, the total intensity exhibits smaller fluctuations around its mean value than before, and reaches the noise level less often.

In summary, we have analyzed the correlation properties of the LP mode intensities of a VCSEL operating in the LFF regime, unveiling a combination of in-phase and partial antiphase pulsating dynamics. The relative proportion of these two correlation properties explains the shape of the statistics of the total intensity, which may be either monotonically decaying from the noise level or peaked around its mean value. We have further shown that the nonlinear gain self-saturation of the lasing transition has a strong influence on the intensity statistics.

[1] K.D. Choquette, D.A. Richie, and R.E. Leibenguth, Appl. Phys. Lett. **64**, 2062 (1994).

[2] Y.C. Chung and Y.H. Lee, IEEE Photonics Technol. Lett. **3**, 597 (1991).

[3] S. Jiang, M. Dagenais, R.A. Morgan, and K. Kojima, Appl. Phys. Lett. **63**, 3545 (1993).

[4] P. Besnard, F. Robert, M.L. Chares, and G.M. Stephan, Phys. Rev. A **56**, 3191 (1997).

[5] N.A. Loiko, A.V. Naumenko, and N.B. Abraham, Quantum Semiclassic. Opt. **10**, 125 (1998).

[6] M. Sciamanna, F. Rogister, O. Deparis, P. Mégret, M. Blondel, and T. Erneux, Opt. Lett. **27**, 261 (2002); **27**, 875(E) (2002).

[7] M. Sciamanna, T. Erneux, F. Rogister, O. Deparis, P. Mégret, and M. Blondel, Phys. Rev. A **65**, 041801(R) (2002).

[8] T. Erneux, A. Gavrielides, and M. Sciamanna, Phys. Rev. A **66**, 033809 (2002).

[9] I. Fischer, T. Heil, and W. Elsäber, in *Nonlinear Laser Dynamics: Concepts, Mathematics, Physics, and Applications International Spring School*, edited by B. Krauskopf and D. Lenstra, AIP Conf. Proc. 548 (AIP, Melville, New York, 2000), pp. 218–237.

[10] C. Masoller and N.B. Abraham, Phys. Rev. A **59**, 3021 (1999).

[11] M. Giudici, S. Balle, T. Ackemann, S. Barland, and J.R. Tredicce, J. Opt. Soc. Am. B **16**, 2114 (1999).

[12] M. Sciamanna, C. Masoller, N.B. Abraham, F. Rogister, P. Mégret, and M. Blondel, J. Opt. Soc. Am. B **20**, 37 (2003).

[13] M. San Miguel, Q. Feng, and J.V. Moloney, Phys. Rev. A **52**, 1728 (1995).

[14] J. Martin-Regalado, F. Prati, M. San Miguel, and N.B. Abraham, IEEE J. Quantum Electron. **33**, 765 (1997).

[15] F. Prati, P. Caccia, and F. Castelli, Phys. Rev. A **66**, 063811 (2002).

[16] R. Lang and K. Kobayashi, IEEE J. Quantum Electron. **QE-16**, 347 (1980).

[17] J.Y. Law and G.P. Agrawal, IEEE J. Sel. Top. Quantum Electron. **3**, 353 (1997).

[18] G. Vaschenko, M. Giudici, J.J. Rocca, C.S. Menoni, J. Tredicce, and S. Balle, Phys. Rev. Lett. **81**, 5536 (1998).

[19] E.A. Viktorov and P. Mandel, Phys. Rev. Lett. **85**, 3157 (2000).

[20] F. Rogister, P. Megret, O. Deparis, and M. Blondel, Phys. Rev. A **62**, 061803(R) (2000).

[21] D. Sukow, J.R. Gardner, and D.J. Gauthier, Phys. Rev. A **56**, R3370 (1997).

[22] T. Ackemann and M. Sondermann, Appl. Phys. Lett. **78**, 3574 (2001).